Received: 5 August 2021 | Revised: 28 September 2021 | Accepted: 21 October 2021

DOI: 10.1002/jcla.24085

RESEARCH ARTICLE

WILEY

Drug metabolism-related eight-gene signature can predict the prognosis of gastric adenocarcinoma

Hong-mei Yin[1] | Qiong He[2] | Jia Chen[1] | Zhen Li[1] | Wanli Yang[1] | Xiaobo Hu[1]

[1]Department of Clinical Laboratory, Longhua Hospital Affiliated to Shanghai University of Traditional Chinese Medicine, Shanghai, China

[2]Pathology Department, Fudan University Shanghai Cancer Center, Shanghai, China

Correspondence
Xiaobo Hu, Department of Clinical Laboratory, Longhua Hospital Affiliated to Shanghai University of Traditional Chinese Medicine, No. 725, South Wanping Road, Shanghai 200032, China.
Email: xiaobohu18@163.com

Abstract

Background: Metabolic abnormalities in patients with gastric adenocarcinoma lead to drug resistance and poor prognosis. Therefore, this study aimed to explore biomarkers that can predict the prognostic risk of gastric adenocarcinoma by analyzing drug metabolism-related genes.

Methods: The RNA-seq and clinical information on gastric adenocarcinoma were downloaded from the UCSC and gene expression omnibus databases. Univariate and least absolute shrinkage and selection operator regression analyses were used to identify the prognostic gene signature of gastric adenocarcinoma. The relationships between gastric adenocarcinoma prognostic risk and tumor microenvironment were assessed using CIBERSORT, EPIC, QUANTISEQ, MCPCounter, xCell, and TIMER algorithms. The potential drugs that could target the gene signatures were predicted in WebGestalt, and molecular docking analysis verified their binding stabilities.

Results: Combined with clinical information, an eight-gene signature, including *GPX3*, *ABCA1*, *NNMT*, *NOS3*, *SLCO4A1*, *ADH4*, *DHRS7*, and *TAP1*, was identified from the drug metabolism-related gene set. Based on their expressions, risk scores were calculated, and patients were divided into high- and low-risk groups, which had significant differences in survival status and immune infiltrations. Risk group was also identified as an independent prognostic factor of gastric adenocarcinoma, and the established prognostic and nomogram models exhibited excellent capacities for predicting prognosis. Finally, miconazole and niacin were predicted as potential therapeutic drugs for gastric adenocarcinoma that bond stably with *NOS3* and *NNMT* through hydrogen interactions.

Conclusions: This study proposed a drug metabolism-related eight-gene signature as a potential biomarker to predict the gastric adenocarcinoma prognosis risks.

KEYWORDS
drug metabolism, gastric adenocarcinoma, immune microenvironment, molecular docking, prognostic model

Hongmei Yin and Qiong He should be regarded as co-first authors.

1 | INTRODUCTION

Gastric adenocarcinoma is a life-threatening malignancy of the gastrointestinal tract and has become the third leading cause of cancer death globally. Of all the gastric cancers, approximately 90%–95% are gastric adenocarcinomas.[1] In 2018, more than one million new cases were confirmed, the majority of which were locally advanced at the time of diagnosis.[2] The 5-year survival rate of advanced or metastatic gastric adenocarcinoma is less than 30%.[3] The incidence of local recurrence or distant metastasis of gastric cancer after surgery remains at 40%–70%, even with surgical intervention, radiotherapy, chemotherapy, and other treatment strategies, along with a certain degree of side effects after radiotherapy and chemotherapy.[4] Therefore, numerous studies have been conducted to explore prognostic biomarkers in an attempt to improve the clinical outcome of patients with gastric adenocarcinoma. Among them, Yao and Ren et al. evaluated the importance of immune microenvironment-related genes in gastric adenocarcinoma prognosis by mining public databases [5,6]. However, a more comprehensive understanding of tumorigenesis mechanisms and the exploration of potential prognostic biomarkers from multiple perspectives are still required.

Metabolic abnormalities are the primary cause of drug resistance in patients with gastric adenocarcinoma, and current studies have provided profound insights into the metabolic changes of gastric adenocarcinoma and discussed their possible regulatory mechanisms.[7] A related genome-wide profile analysis identified several important gastric cancer biomarkers that were significantly associated with drug metabolism pathways.[8] The long non-coding RNA MACC1-AS1, a biomarker related to gastric cancer prognosis, was reported to regulate disease metabolism through enhanced glycolysis and antioxidant capacity.[9] Furthermore, ectopic expression of S100P has been found to correlate with proliferation and increased drug resistance in gastric cancer cells.[10] A bioinformatics study found that the differentially expressed genes (DEGs), including *ASPN*, *COL1A1*, *FN1*, *VCAN*, and *MUC5AC*, in gastric cancer were significantly associated with survival prognoses of patients and were predominantly enriched in drug metabolism pathways.[11] Although these genes were found to be involved in drug metabolism pathways, few studies have systematically reported drug metabolism-related drugs and thoroughly explored their prognostic values.

Therefore, the current study aimed to identify genes that are significantly associated with gastric adenocarcinoma prognosis from drug metabolism-related gene sets. Based on the expression of these genes, we constructed a prognostic model and explored the predictive performance of the model through internal and external validation. Furthermore, we predicted the drugs that could target these genes and performed a molecular docking analysis to verify their binding. Additionally, multiple databases were used to investigate the relationship between the prognostic risk of gastric adenocarcinoma and the immune microenvironment. The workflow of the study is shown in Figure S1. The feature genes proposed in this study may be potential therapeutic markers, resulting in improved clinical outcomes in patients.

2 | MATERIALS AND METHODS

2.1 | Data acquisition

RNA-seq data of gastric adenocarcinoma and related clinical information, including tumor stage, family history, lymph node examined count, neoplasm histologic grade, primary diagnosis, resection or biopsy site, disease type, overall survival (OS), and OS duration were downloaded from the UCSC Xena (https://toil.xenahubs.net) platform.[12] A total of 32 paracancerous samples and 375 tumor samples were included in this study, and 348 gastric adenocarcinoma samples with prognostic information were enrolled to develop a prognostic model. Furthermore, expression data and clinical information of 65 gastric adenocarcinoma samples in the microarray dataset GSE13861 were obtained from the Gene Expression Omnibus (GEO, http://www.ncbi.nlm.nih.gov/geo/) database.[13] GSE13861 was detected using the GPL6884 Illumina HumanWG-6 v3.0 Expression BeadChip and was used as the validation set.

2.2 | Analysis of drug metabolism-related genes

Based on published articles[14] and The Cancer Genome Atlas (TCGA) database, a total of 228 drug metabolism-related genes were matched. Using the empirical Bayes method provided by the limma package (v3.10.3, http://www.bioconductor.org/packages/2.9/bioc/html/limma.html),[15] drug metabolism-related DEGs between tumor and paracancerous samples were identified with *p*-values adjusted by Benjamini & Hochberg method < 0.05, and $|\log \text{fold-change}| > 0.5$ as thresholds.

2.3 | Enrichment analysis and protein-protein-interaction (PPI) network construction

Gene ontology (GO) functions and Kyoto Encyclopedia of Genes and Genomes (KEGG) pathways of drug metabolism-related DEGs were enriched in DAVID v6.8 (http://david.ncifcrf.gov/) [16,17]. GO and KEGG terms with p-value < 0.05, and gene count ≥2 were selected with significant correlation. Moreover, the STRING database (v11.0, http://string-db.org/)[18] was used to analyze the relationship between proteins coded by drug metabolism-related DEGs, and the PPI network was visualized using Cytoscape (v3.6.1, http://cytoscape.org/).[19]

2.4 | Screening of drug metabolism-related prognostic DEGs

Based on the drug metabolism-related DEGs obtained above and the survival information of gastric adenocarcinoma samples, univariate Cox regression analysis was performed to select drug

metabolism-related prognostic DEGs using the survival package (v2.41–1, http://bioconductor.org/packages/survivalr/) in R3.6.1.[20] DEGs with a p-value < 0.05 were determined to be significantly correlated with prognosis.

2.5 | Construction and validation of the prognostic model

By utilizing the prognostic information of gastric adenocarcinoma samples in the training set and the expression values of drug metabolism-related prognostic DEGs in each sample, genes were further selected as the optimized gene set using the least absolute shrinkage and selection operator (LASSO) regression analysis in the glmnet package (v2.0–18, http://cran.r-project.org/web/packages/glmnet/index.html) [21,22]. The risk score of each sample was then calculated as follows:

$$Risk\ score = \sum \beta_{gene} \times Exp_{gene}$$

where β_{gene} indicates the LASSO regression coefficient of gene signature, and Exp_{gene} indicates their expression levels in gastric adenocarcinoma samples. To verify the effectiveness of the prognostic model, the risk scores of the samples in GSE13861 were calculated. The samples were then grouped into high- and low-risk groups based on the median risk score. Kaplan-Meier (KM) curves were created to analyze the difference in survival status between the two groups.

2.6 | Feature analysis of gene signature

The expression cutoff value of each gene signature in the training set was obtained to determine the optimal cutoff point calculated by the Survminer package of R3.6.1 (v0.4.3). KM analysis was then performed to evaluate the difference in survival prognosis between samples in the high- and low-expression groups. A heatmap was created to observe the relationships between the expression level, risk score, and clinical characteristics of each gastric adenocarcinoma sample.

2.7 | Statistical analysis of clinical features among risk groups

In the training set, the chi-squared test in R3.6.1 was used for statistical analysis and comparison of categorical variables, including TNM classification, tumor stage, family history, neoplasm histologic grade, primary diagnosis, resection or biopsy site, and disease type, between risk groups. The t test was used for continuous variables, including age and lymph node examined count.

2.8 | Immune microenvironment analysis between risk groups

In the current study, CIBERSORT (https://cibersort.stanford.edu/index.php) [23,24], EPIC (https://gfellerlab.shinyapps.io/EPIC_1-1/),[25] QUANTISEQ,[26] MCP-counter (https://github.com/ebecht/MCPcounter),[27] xCell (https://xcell.ucsf.edu/),[28] and TIMER (https://cistrome.shinyapps.io/timer)[29] were used to estimate immune cell infiltration among risk groups. The Wilcoxon test was used to analyze the difference between the two groups and a heatmap was created accordingly. Furthermore, the ESTIMATE algorithm[30] was used to assess the stromal and immune scores of gastric adenocarcinoma samples, and the t test was applied to analyze the difference, followed by generation of a box plot.

2.9 | Differential pathway analysis between risk groups

Gene Set Enrichment Analysis (GSEA, v3.0) software was used for pathway enrichment with c2.cp.kegg.v7.1.symbols.gmt in MSigDB v7.1 (http://software.broadinstitute.org/gsea/msigdb/index.jsp)[31] as an enrichment background. Then, the differences in enriched pathways were analyzed between risk groups with a false discovery rate (FDR) < 0.05.

2.10 | Analysis of independent prognostic factors and construction of a nomogram prediction model

To determine whether the prognostic model could be used as an independent prognostic factor, univariate Cox regression analysis was performed on age, sex, tumor stage, family history, neoplasm histologic grade, disease type, and lymph node examined count. Variables with p-values < 0.05 were selected for multivariate Cox regression analysis, followed by a further selection of statistical significance at $p < 0.05$. A nomogram model was created to predict the 1-, 2-, 3-, and 5-year survival probabilities of gastric adenocarcinoma patients according to the multivariate Cox regression analysis results. Calibration curves were generated to verify model accuracy.

2.11 | Drug enrichment prediction of gene signature

Based on the obtained genes, the WebGestalt database (http://www.webgestalt.org/option.php)[32] was used for drug enrichment prediction using over-representation analysis. Drugs with $p < 0.05$ were selected as candidate drugs that could bind with the genes. Based on the prognostic effect of the gene signature, drugs that

function as inhibitors or inducers were selected. Finally, the binding stabilities between candidate inhibitors or induced drugs and related target genes were validated by molecular docking using AutoDock 4.2.6.

3 | RESULTS

3.1 | Analysis of drug metabolism-related DEGs of gastric adenocarcinoma

Differential analysis was performed between gastric adenocarcinoma samples and paracancerous samples based on 228 matched drug metabolism-related genes. The volcano plot (Figure 1A) shows the 77 obtained drug metabolism-related DEGs. Then, enrichment analysis was performed on these drug metabolism-related DEGs, and 64 biological processes (BP), 13 cellular components (CC), 47 molecular functions (MF), and 21 KEGG pathways were obtained. The bubble charts of Figure 1B display the top 10 GO and KEGG terms, ranked by *p*-values. The results showed that these DEGs were primarily enriched in GO-BP of several metabolic processes, GO-CC of TAP complex and host cell, GO-MF of aldehyde dehydrogenase activity, and in KEGG pathways of drug metabolism, xenobiotic metabolism, and chemical carcinogenesis. The interactions of these proteins coded by DEGs were then analyzed, and a PPI network was created, as shown in Figure 1C. This PPI network contained 66 drug metabolism-related DEGs and 309 relation pairs. Among these nodes, *UGT1A1*, *CYP2B6*, and *CYP3A4* had a larger degree.

3.2 | Screening of gene signature of gastric adenocarcinoma

Combined with the prognostic information of gastric adenocarcinoma samples, a univariate Cox regression analysis was

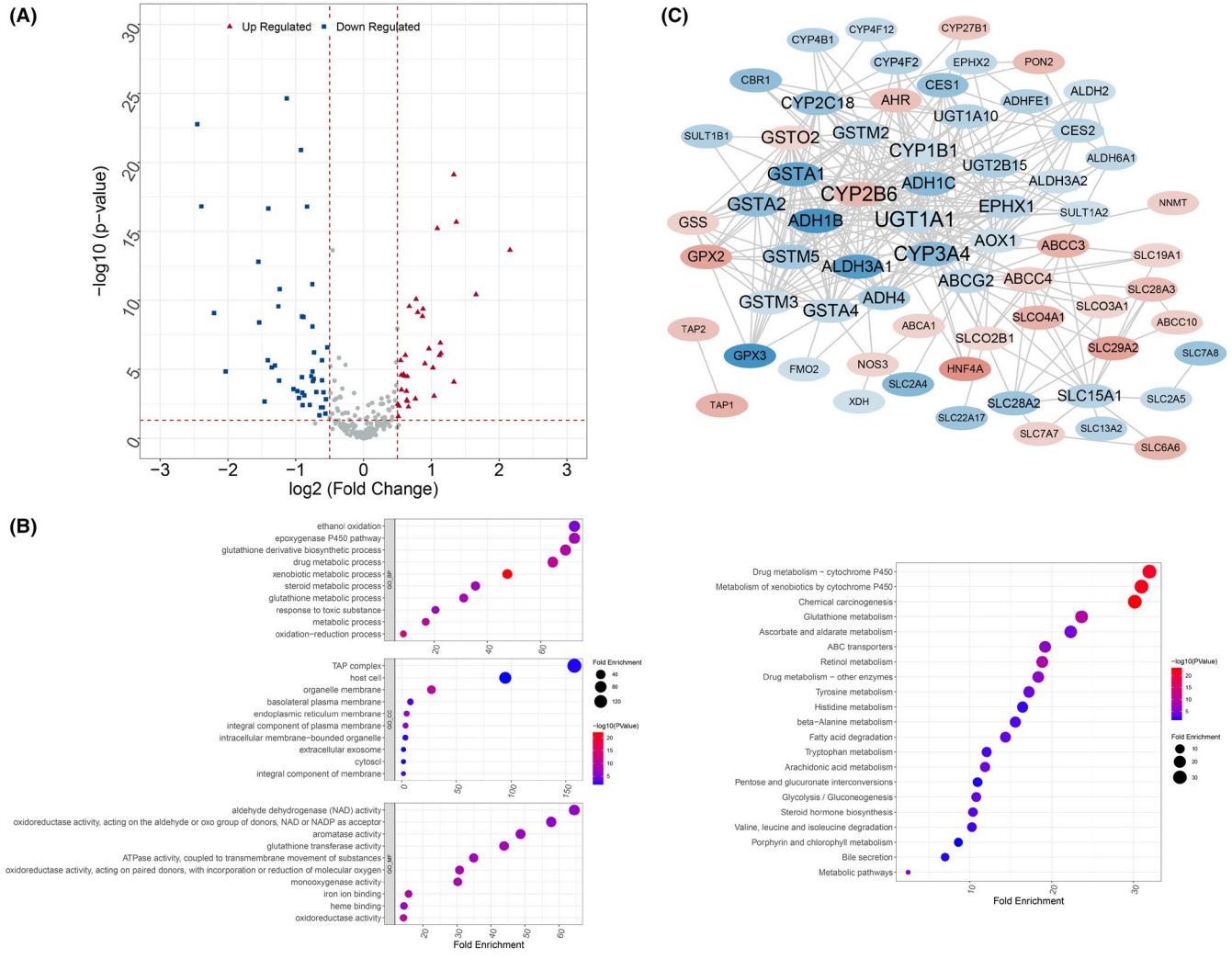

FIGURE 1 Analysis of drug metabolism-related DEGs of gastric adenocarcinoma. (A) The volcano plot shows drug metabolism-related DEGs between gastric adenocarcinoma samples and paracancerous samples; (B) GO functions and KEGG pathway enrichment analyses of drug metabolism-related DEGs; (C) The protein-protein-interaction network created based on proteins coded by drug metabolism-related DEGs

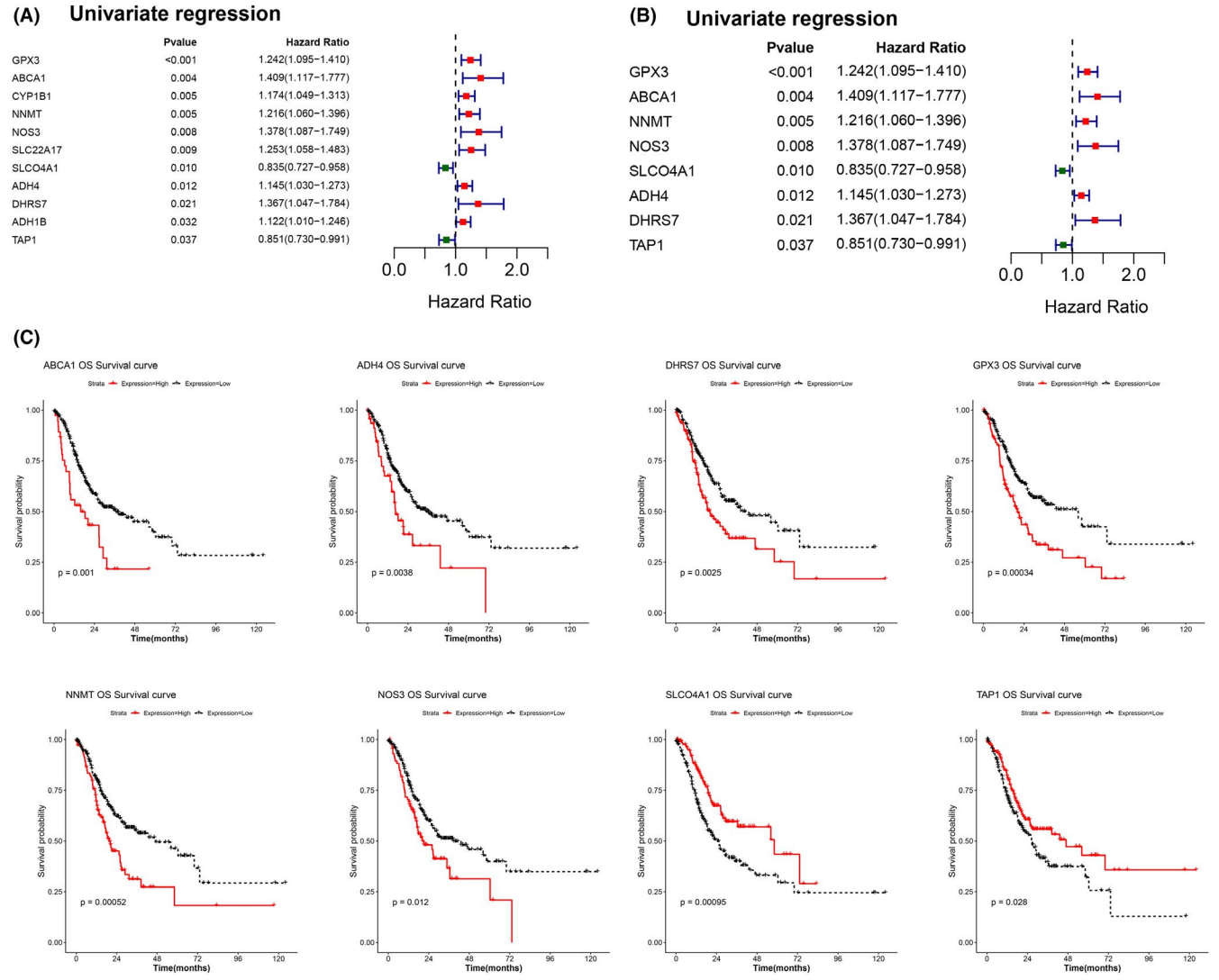

FIGURE 2 Screening of gene signature of gastric adenocarcinoma. (A) The forest map shows the prognostic DEGs selected from the univariate Cox regression analysis; (B) the forest map shows the gene signature of gastric adenocarcinoma screened by the multivariate regression analysis; (C) KM curves show the survival differences between patients with different expression levels of these genes

performed, and 11 drug metabolism-related prognostic DEGs were selected with $p < 0.05$, as shown in Figure 2A. Then, LASSO regression analysis was performed to select the optimized gene set, and an eight-gene signature was identified, including *GPX3*, *ABCA1*, *NNMT*, *NOS3*, *SLCO4A1*, *ADH4*, *DHRS7*, and *TAP1*. Their prognostic effects are shown in Figure 2B, and only *SLCO4A1* and *TAP1* were considered protective factors with hazard ratios <1. Based on the expression cutoff of these genes in the training set, samples were separated into high- and low-expression groups. The KM curves in Figure 2C illustrated that patients with high *GPX3*, *ABCA1*, *NNMT*, *NOS3*, *ADH4*, and *DHRS7* expressions had worse survival status, whereas high *SLCO4A1* and *TAP1* expressions were significantly associated with better prognoses.

3.3 | Establishment and validation of the prognostic model

Using the LASSO regression coefficients of each gene obtained above, the risk scores of each sample were calculated, and a prognostic model was created. Based on the median value of the risk score, the samples were grouped into high- and low-risk groups. The expression distributions of these genes in the two groups were visualized using a heatmap (Figure 3A). The results suggested that the expression distribution of genes in the risk groups was different. To validate the model efficiency in the training set, we found that the prognostic risk of patients increased along with increased risk scores (Figure 3B). The KM curve (Figure 3C) demonstrated that patients in the high-risk groups had a worse survival status. Receiver operator

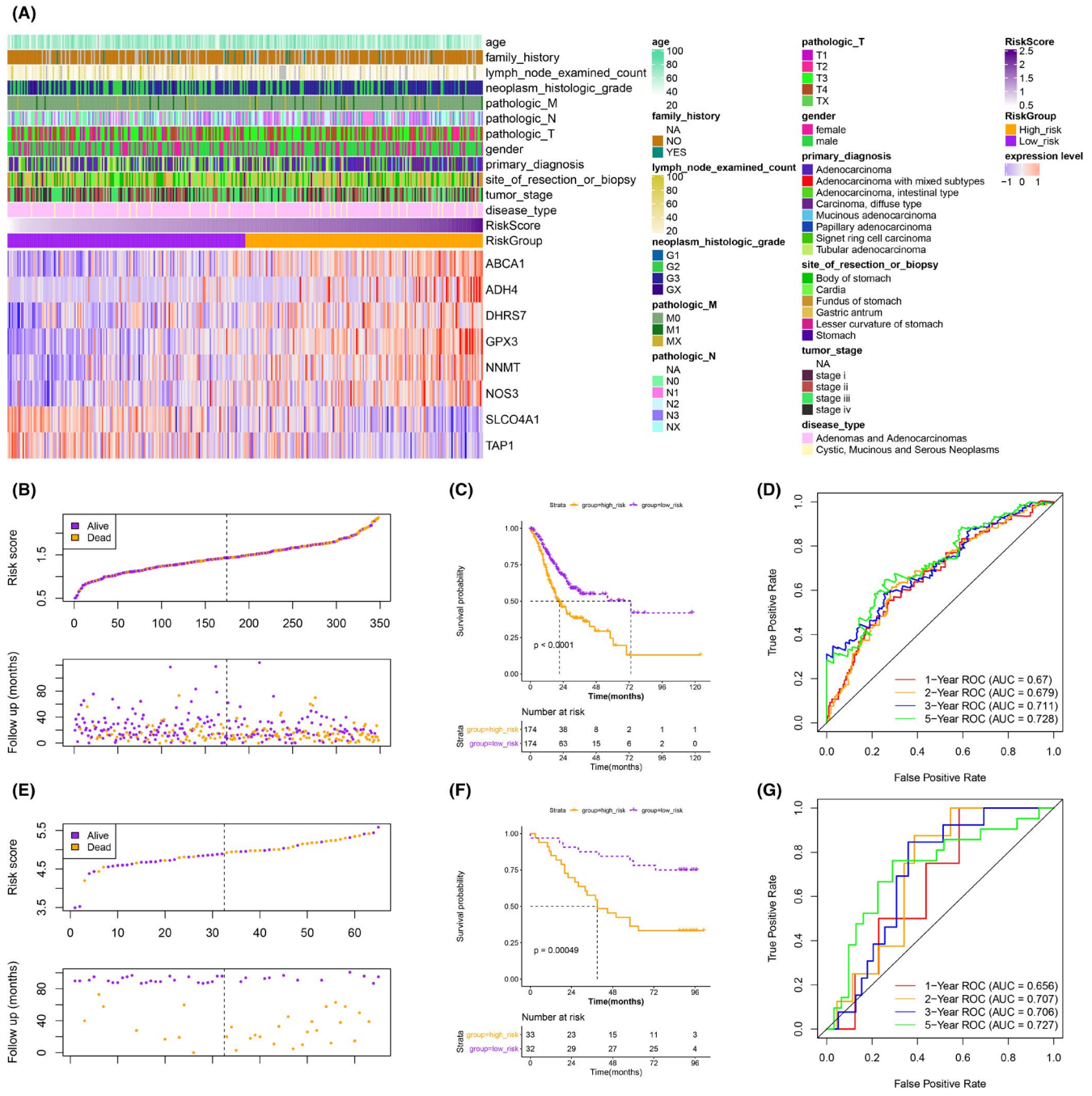

FIGURE 3 Construction and validation of the prognostic model. (A) The heatmap shows the expression distribution of genes in high- and low-risk groups; Model validation in the training set (B–D) and the GSE13861 validation dataset (E–G); (B and E) the distribution of survival time on risk scores; (C and F) KM curves show the survival difference between the two groups; (D and G) Receiver operator characteristic curves show the model accuracy in predicting 1-, 2-, 3-, and 5-year prognoses

characteristic (ROC) curves (Figure 3D) were created to verify model accuracy, and it was observed that the prognostic model had superior performance in predicting 1-, 2-, 3-, and 5-year survival prognoses with area under the curves (AUCs) of 0.67, 0.679, 0.711, and 0.728, respectively. The prognostic model was further validated using the GSE13861 dataset (Figure 3E–G). Similarly, as the risk score increased, the number of deaths increased. Meanwhile, patients in the high- and low-risk groups had significant differences in survival time, and the model accuracy was proven in the validation set with all AUCs in ROC curves over 0.65. These results indicated a significant association between the risk grouping and actual outcomes.

3.4 | Difference of clinical characteristics between risk groups

The clinical information of the high- and low-risk groups was compared, as shown in Table 1. The results suggested that the two

TABLE 1 The statistics of clinical features in the high-risk and low-risk groups

Subgroups	Low risk	High risk	*p*-Value
Age (mean ± SD)	66.0 ± 10.1	64.6 ± 10.6	2.058E−01
Lymph node examined count	26.5 ± 20.9	19.2 ± 15.1	**4.264E−04**
Family history			5.088E−01
Yes	9	6	
No	133	129	
NA	32	39	
Tumor stage			**3.544E−04**
I	1	12	
II	34	54	
III	56	74	
IV	70	22	
NA	12	12	
Neoplasm histologic grade			**3.463E−03**
G1	3	6	
G2	77	46	
G3	89	118	
GX	5	4	
Pathologic M			8.204E−02
M0	161	150	
M1	6	16	
MX	7	8	
Pathologic N			**3.294E−03**
N0	65	38	
N1	39	53	
N2	39	32	
N3	29	42	
NX	2	7	
NA	0	2	
Pathologic T			**6.183E−04**
T1	15	1	
T2	38	36	
T3	79	80	
T4	42	53	
TX	0	4	
Primary diagnosis			**1.223E−03**
Adenocarcinoma	55	62	
Adenocarcinoma with mixed subtypes	0	1	
Adenocarcinoma, intestinal type	40	33	
Carcinoma, diffuse type	20	39	
Mucinous adenocarcinoma	6	13	
Papillary adenocarcinoma	4	1	
Signet ring cell carcinoma	5	7	
Tubular adenocarcinoma	44	18	

(Continues)

TABLE 1 (Continued)

Subgroups	Low risk	High risk	*p*-Value
Site of resection or biopsy			7.366E−01
Body of stomach	46	38	
Cardia	44	40	
Fundus of stomach	18	22	
Gastric antrum	59	68	
Lesser curvature of stomach	1	0	
Stomach	6	6	
Disease type			1.941E−01
Adenomas and Adenocarcinomas	162	154	
Cystic, Mucinous and Serous Neoplasms	12	20	

Note: Bold *p*-value < 0.05 indicates statistical significance.
Abbreviations: NA, not available; SD, standard division.

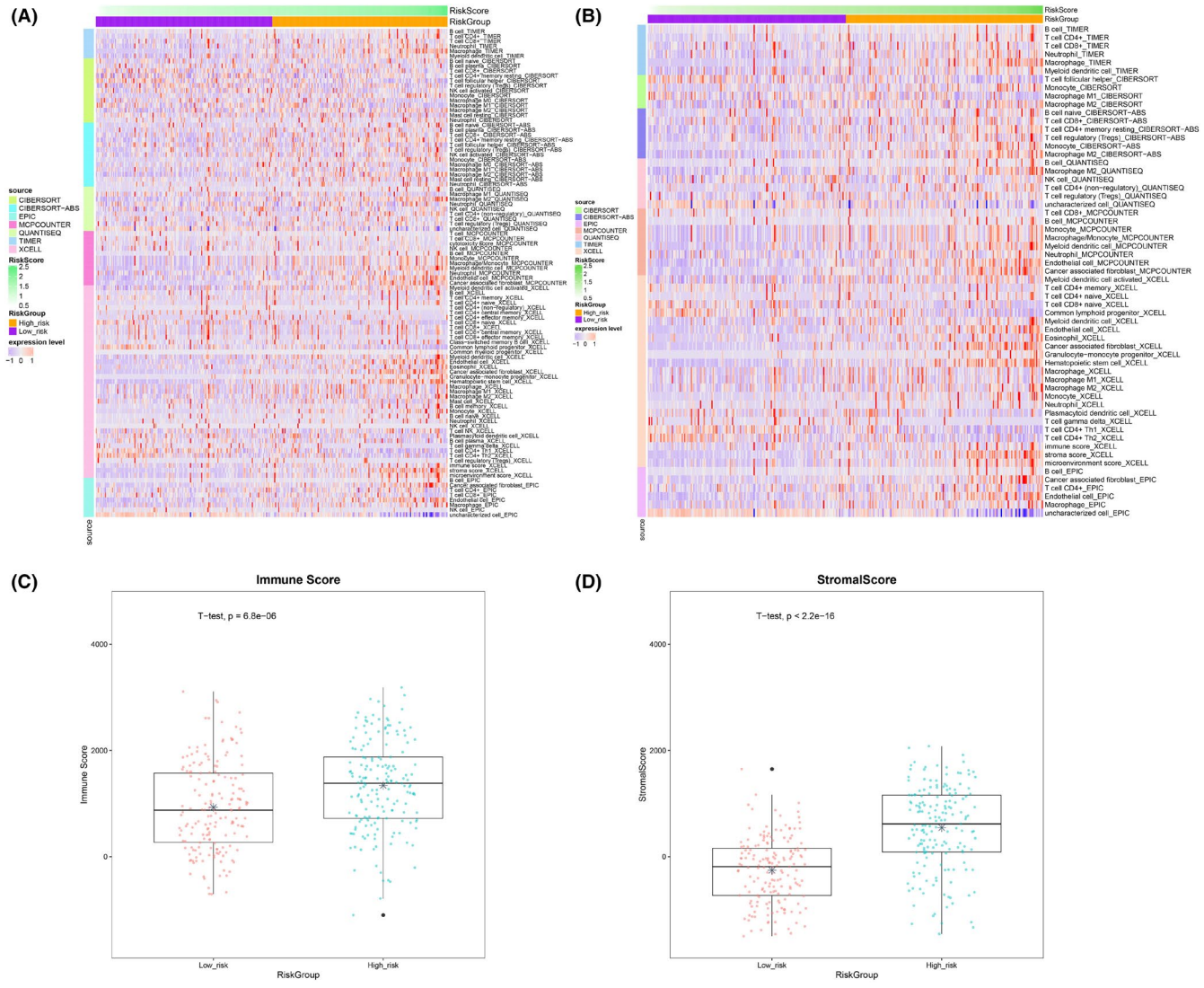

FIGURE 4 Estimation of immune cell infiltration abundance in high- and low-risk groups. (A) The infiltration abundances of immune and stromal cells estimated by CIBERSORT, EPIC, QUANTISEQ, MCPCounter, xCell, and TIMER algorithms; (B) the heatmap shows 59 immune microenvironment-related cells with $p < 0.05$; (C) the difference in immune scores between high- and low-risk groups; (D) the difference in stromal scores between high- and low-risk groups

groups had significant differences in lymph node examined count, tumor stage, neoplasm histologic grade, pathologic N, pathologic T, and primary diagnosis.

3.5 | Difference of immune microenvironment between risk groups

Based on CIBERSORT, EPIC, QUANTISEQ, MCPCounter, xCell, and TIMER algorithms, the relative infiltration abundances of immune and stromal cells were estimated. The infiltration abundance of immune cells is shown in Figure 4A. Then, by comparing the differences between risk groups, 59 immune microenvironment-related cells ($p < 0.05$) were screened out, as shown in Figure 4B. Immune and stromal scores were calculated for each sample, and significant differences between risk groups were visualized using box plots (Figure 4C,D).

3.6 | GSEA pathway enrichment analysis among risk groups

The KEGG pathways of high- and low-risk groups were analyzed using GSEA. By setting the threshold of FDR < 0.05, the high-risk group significantly enriched 25 KEGG pathways with a normalized enrichment score (NES) >0. Furthermore, 11 significant pathways were enriched in the low-risk group, with an NES < 0. The enriched pathways of these two groups are shown in Table 2.

3.7 | Analysis of independent prognostic factors and establishment of a nomogram model

To further identify the independent prognostic factors, age, sex, tumor stage, family history, neoplasm histologic grade, TNM classification, disease type, and lymph node examined count were incorporated into the univariate Cox regression analysis (Figure 5A). Variables with *p*-values < 0.05 were then selected for multivariate Cox regression analysis. Finally, the risk group, pathologic N, and pathologic M were identified as independent prognostic factors (Figure 5B). A nomogram model was established to predict 1-, 2-, 3-, and 5-year survival probabilities (Figure 5C), and calibration curves were created to verify model accuracy. Figure 5D shows that the predicted probabilities of 2-, 3-, and 5-year OS were similar to the actual OS, thereby suggesting an excellent prediction accuracy of the nomogram model.

3.8 | Molecular docking analysis of predicted drugs and related targets

Drug prediction enrichment analysis was performed on an eight-gene signature, and 30 drugs were predicted to target 7 genes. Among them, high *ABCA1*, *NNMT*, and *NOS3* expression levels were correlated with poor prognoses, and their related inhibitors or binder's glyburide, niacin, and miconazole, respectively, were selected for molecular docking analyses. The binding results of glyburide-*ABCA1*, miconazole-*NOS3*, and niacin-*NNMT* complexes are shown in Figure 6A–C, respectively. As a result, miconazole bonded with the PHE-473 residue of *NOS3* by a hydrogen bond with a length of 2.5 Å. Moreover, the small molecular ligand niacin bonded with ARG-30 and SER-32 residues of the receptor *NNMT* through hydrogen bond interactions. These findings illustrated that these ligand-receptor complexes were in a stable state of binding.

4 | DISCUSSION

Gastric adenocarcinoma ranks fifth among the most prevalent malignancies worldwide, and the development of drug resistance because of metabolic disorders is one of the reasons for poor prognosis.[1] Therefore, by mining TCGA and GEO, we identified eight prognostic genes, namely *GPX3*, *ABCA1*, *NNMT*, *NOS3*, *SLCO4A1*, *ADH4*, *DHRS7*, and *TAP1* from the drug metabolism-related gene set using univariate and LASSO regression analyses. Then, a prognostic model was constructed, and patients were grouped into high- and low-risk groups. Survival analyses showed that patients in the high-risk group had worse prognoses, while the ROC curves showed that the prognostic model had good predictive performance in both the training and validation sets with AUCs > 0.65. Furthermore, the risk group was identified as an independent prognostic factor, and the established nomogram model exhibited good accuracy in predicting 1-, 2-, 3-, and 5-year survival probabilities.

Among the eight genes, we found that *SLCO4A1* and *TAP1* were protective factors for gastric adenocarcinoma prognosis, whereas high *GPX3*, *ABCA1*, *NNMT*, *NOS3*, *ADH4*, and *DHRS7* expressions were significantly associated with poor prognoses. It has been reported that in gastric cancer patients over 60 years of age, *GPX3* hypermethylation was significantly correlated with a shorter time to tumor recurrence.[33] Meanwhile, Wang et al. believed that *GPX3* is a risk factor for gastric cancer, and the intron single nucleotide polymorphism of *GPX3* may alter gastric cancer risk by affecting gene expression levels.[34] Therefore, we speculated that the risk role of *GPX3* in gastric adenocarcinoma prognosis may be closely related to changes in gene epigenetics. As for *NNMT*, related studies found that high *NNMT* expression in stromal cells may predict an unfavorable postoperative prognosis for gastric carcinoma.[35] *NNMT* is known to act as a negative predictor for gastric carcinoma prognosis and is correlated with immune infiltrates [36,37]. These findings confirmed our results, and upregulated *NNMT* in gastric cancer cells may promote the occurrence of epithelial-mesenchymal transition by activating TGF-β1/SMAD signaling,[38] thereby leading to tumor recurrence and metastasis. A pan-cancer analysis found that increased *NOS3* expression in gastric adenocarcinoma may lead to poor prognosis through several typical cancer-related pathways.[39]

TABLE 2 Enrichment GSEA pathways of high- and low-risk groups

Terms (High-risk)	NES	FDR *p*-Value
Focal adhesion	2.068	0.040
Regulation of actin cytoskeleton	2.054	0.024
Hypertrophic cardiomyopathy HCM	2.031	0.021
Complement and coagulation cascades	2.023	0.018
Vascular smooth muscle contraction	2.004	0.018
Glycosphingolipid biosynthesis ganglio series	1.992	0.018
Calcium signaling pathway	1.976	0.018
KEGG dilated cardiomyopathy	1.965	0.019
Arrhythmogenic right ventricular cardiomyopathy ARVC	1.964	0.017
ECM receptor interaction	1.934	0.023
GAP junction	1.923	0.025
Leukocyte transendothelial migration	1.920	0.024
Vasopressin regulated water reabsorption	1.861	0.040
TGF-β signaling pathway	1.851	0.041
Neuroactive ligand-receptor interaction	1.851	0.039
Melanogenesis	1.846	0.038
Pathogenic escherichia coli infection	1.833	0.041
Cell adhesion molecules cams	1.829	0.040
MAPK signaling pathway	1.821	0.041
Prion diseases	1.817	0.041
Adherens junction	1.802	0.045
Glycosaminoglycan biosynthesis chondroitin sulfate	1.801	0.043
Melanoma	1.788	0.046
Hematopoietic cell lineage	1.775	0.049
Axon guidance	1.770	0.049
Terms (Low-risk)	**NES**	**FDR *p*-Value**
Spliceosome	−2.117	0.015
DNA replication	−1.966	0.039
RNA degradation	−1.946	0.032
Base excision repair	−1.896	0.040
Homologous recombination	−1.891	0.035
Aminoacyl tRNA biosynthesis	−1.886	0.031
One carbon pool by folate	−1.876	0.029
Pyrimidine metabolism	−1.870	0.027
Proteasome	−1.868	0.025
Cell cycle	−1.862	0.023
Nucleotide excision repair	−1.800	0.039

Abbreviations: FDR, false discovery rate; GSEA, gene set enrichment analysis; NES, normalized enrichment score.

This finding is consistent with our results; however, how *NOS3* influences gastric adenocarcinoma prognosis through cancer-related pathways requires investigation.

The tumor microenvironment significantly contributes to the occurrence, progression, prognosis, and immunotherapy response of gastric adenocarcinoma.[6] Gastric adenocarcinoma is a chronic gastritis caused by *Helicobacter pylori* and is often characterized by the infiltration of immune cells, including granulocytes, macrophages, and T lymphocytes.[40] Therefore, the current study explored the relationship between prognostic risk and immune cell infiltration. Significant differences in the infiltration of 59 immune microenvironment-related cells, such as B cells, T cells, neutrophils, and macrophages were found between the risk groups. Relevant studies have reported that high infiltration of B lymphocytes is beneficial for gastric cancer prognosis.[41] Fristedt and Knief et al. suggested that increased infiltration density of B cells

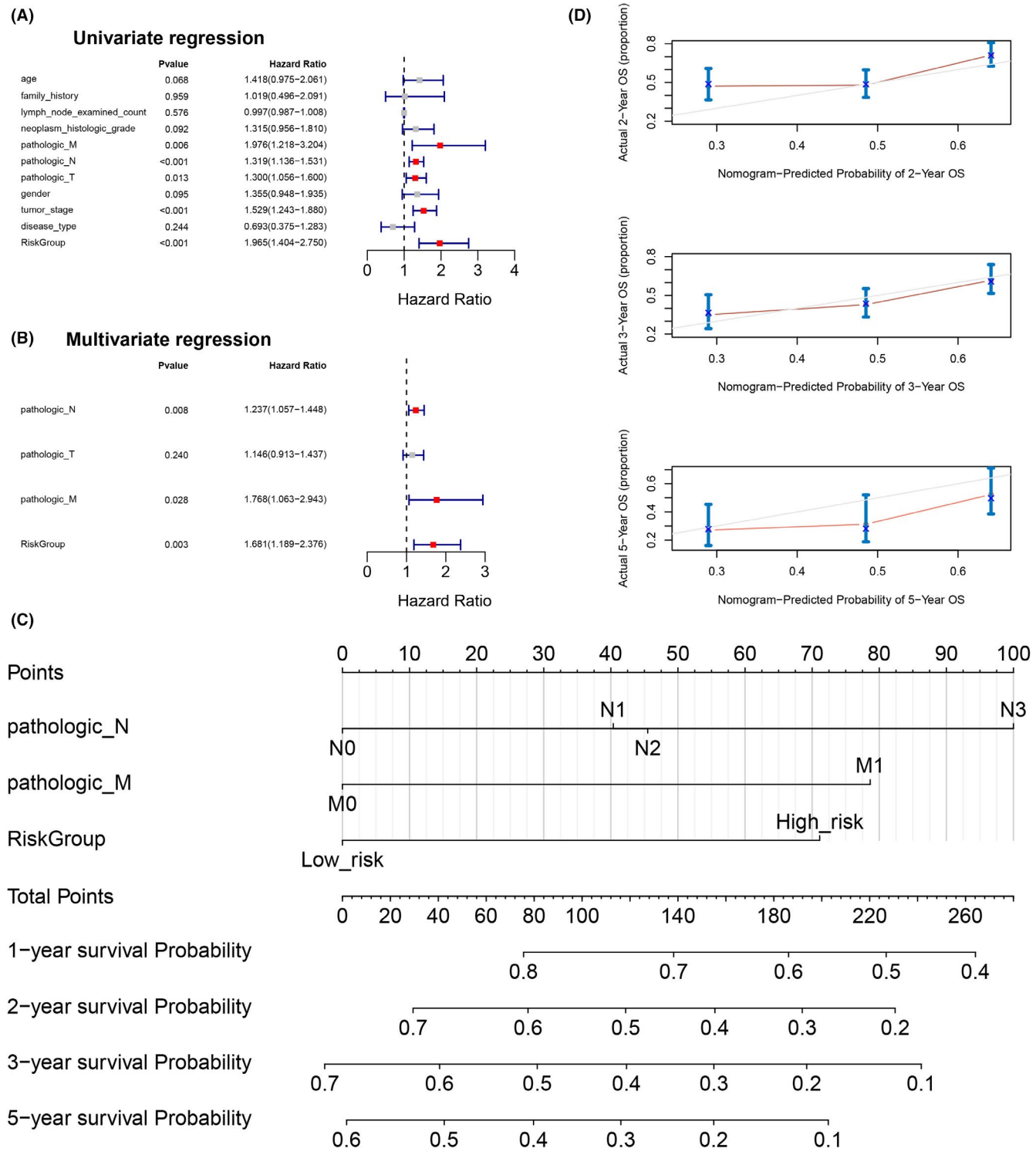

FIGURE 5 Construction and validation of the nomogram model. (A and B) Identification of the independent prognostic factors using univariate and multivariate Cox regression analyses; (C) the establishment of a nomogram model to predict 1-, 2-, 3-, and 5-year survival probabilities; (D) calibration curves were created to verify the accuracy of the nomogram model

or plasma cells was associated with improved prognosis and prolonged OS of esophageal and gastric cancers [42,43]. As for T cells, increased CD8+T cell infiltration was associated with impaired OS, and PD-L1 expression was higher in patients with a higher CD8+T cell density, suggesting a possible mechanism of adaptive immune resistance.[44] Christina et al.[45] reported that the high CD8+T cell density was an adverse prognostic factor for gastric adenocarcinoma patients. However, certain contrasting results suggested that increased CD3+ and CD8+ T lymphocyte infiltrations are associated with improved survival status.[46] The upregulation of

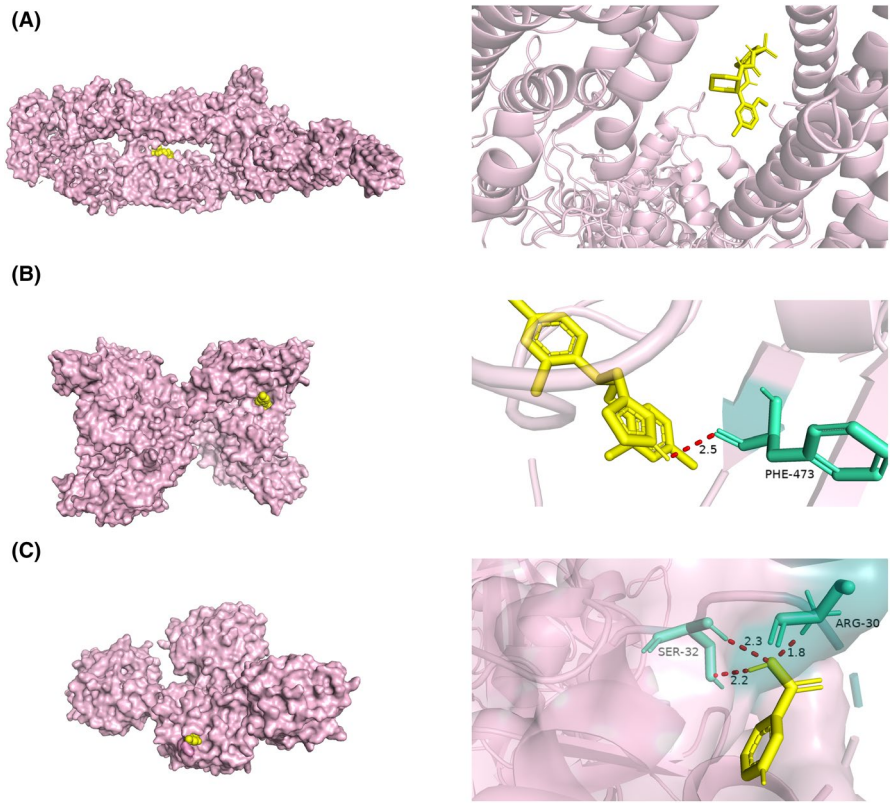

FIGURE 6 Molecular docking analyses of Glyburide-*ABCA1* (A), miconazole-*NOS3* (B), and niacin-*NNMT* (C) complexes. Yellow and pink indicate small molecular ligand and protein receptors, respectively. Green indicates the binding residues, while the red line indicates hydrogen bond interaction

PD-1 and PD-L1 is believed to promote T-cell apoptosis in gastric adenocarcinoma.[47] The association between T cell infiltration and the prognostic risk of gastric adenocarcinoma has been extensively introduced; however, the specific prognostic effects of T cells remain controversial, possibly because of the differences in identified T cell subtype markers and gastric cancer molecular subtypes among different studies.

At the end of this study, we predicted several inhibitors or binders based on prognostic risk genes as potential drugs for gastric adenocarcinoma treatment, and the molecular docking analysis showed that the drug ligand and the protein receptor bond stably in the form of hydrogen bonds. However, our understanding of the therapeutic potential of drugs for gastric adenocarcinoma is limited. In future studies, we will conduct animal experiments to explore whether the molecular mechanism of niacin and miconazole for gastric adenocarcinoma treatment is related to the expression of target genes.

5 | CONCLUSIONS

In summary, this study proposed an eight-gene signature related to drug metabolism as a potential biomarker to predict the prognostic risk of gastric adenocarcinoma patients. The predicted drugs (niacin and miconazole) can stably bind to target genes and have therapeutic potential for gastric adenocarcinoma patients. Additionally, we found a significant correlation between the tumor immune microenvironment and gastric adenocarcinoma prognosis. Our study helps to better understand the relationship between gastric adenocarcinoma prognosis, drug metabolism, and the immune microenvironment.

ACKNOWLEDGEMENTS

Not applicable.

CONFLICT OF INTEREST

The authors declare that they have no competing interests.

AUTHOR CONTRIBUTION

Hongmei Yin and Qiong He conceived and designed the research, and Zhen Li and Jia Chen participated in the acquisition of data. Wanli Yang performed the analysis and interpretation of data. Jia Chen and Wanli Yang participated in the design of the study and performed the statistical analyses. Hongmei Yin, Qiong He, and Xiaobo Hu conceived the study, participated in its design and coordination, and helped draft the manuscript and revised the manuscript for important intellectual content. All authors read and approved the final manuscript.

DATA AVAILABILITY STATEMENT

The raw data supporting the conclusions of this manuscript will be made available by the authors, without undue reservation, to any qualified researcher.

ORCID

Xiaobo Hu https://orcid.org/0000-0001-5467-9512

REFERENCES

1. Zhou L, Huang W, Yu HF, Feng YJ, Teng X. Exploring TCGA database for identification of potential prognostic genes in stomach adenocarcinoma. *Cancer Cell Int*. 2020;20:264.
2. Bray F, Ferlay J, Soerjomataram I, Siegel RL, Torre LA, Jemal A. Global cancer statistics 2018: GLOBOCAN estimates of incidence and mortality worldwide for 36 cancers in 185 countries. *CA Cancer J Clin*. 2018;68(6):394-424.
3. Suzuki H, Oda I, Abe S, et al. High rate of 5-year survival among patients with early gastric cancer undergoing curative endoscopic submucosal dissection. *Gastric Cancer*. 2016;19(1):198-205.
4. Wagner AD, Syn NL, Moehler M, et al. Chemotherapy for advanced gastric cancer. *Cochrane Database Syst Rev*. 2017;8(8):CD004064.
5. Yao K, Wei L, Zhang J, et al. Prognostic values of GPNMB identified by mining TCGA database and STAD microenvironment. *Aging*. 2020;12(16):16238-16254.
6. Ren N, Liang B, Li Y. Identification of prognosis-related genes in the tumor microenvironment of stomach adenocarcinoma by TCGA and GEO datasets. *Biosci Rep*. 2020;40(10):BSR20200980.
7. Kim HK, Choi IJ, Kim CG, et al. A gene expression signature of acquired chemoresistance to cisplatin and fluorouracil combination chemotherapy in gastric cancer patients. *PLoS One*. 2011;6(2):e16694.
8. Fei HJ, Chen SC, Zhang JY, et al. Identification of significant biomarkers and pathways associated with gastric carcinogenesis by whole genome-wide expression profiling analysis. *Int J Oncol*. 2018;52(3):955-966.
9. Zhao Y, Liu Y, Lin L, et al. The lncRNA MACC1-AS1 promotes gastric cancer cell metabolic plasticity via AMPK/Lin28 mediated mRNA stability of MACC1. *Mol Cancer*. 2018;17(1):69.
10. Ge F, Wang C, Wang W, Wu B. S100P predicts prognosis and drug resistance in gastric cancer. *Int J Biol Markers*. 2013;28(4):e387-e392.
11. Jiang K, Liu H, Xie D, Xiao Q. Differentially expressed genes ASPN, COL1A1, FN1, VCAN and MUC5AC are potential prognostic biomarkers for gastric cancer. *Oncol Lett*. 2019;17(3):3191-3202.
12. Goldman MJ, Craft B. Visualizing and interpreting cancer genomics data via the Xena platform. *Nat Biotechnol*. 2020;38(6):675-678. https://doi.org/10.1038/s41587-020-0546-8
13. Barrett T, Wilhite SE, Ledoux P, et al. NCBI GEO: archive for functional genomics data sets--update. *Nucleic Acids Res*. 2013;41(D1):D991-D995.
14. Hu DG, Mackenzie PI, Nair PC, McKinnon RA, Meech R. The expression profiles of ADME genes in human cancers and their associations with clinical outcomes. *Cancers*. 2020;12(11):3369.
15. Smyth GK. Limma: Linear models for microarray data. In Irizarry R, Gentleman R, Dudoit S, Carey V, Huber W eds. *Bioinformatics and Computational Biology Solutions Using R and Bioconductor*. Springer; 2005.
16. da Huang W, Sherman BT, Lempicki RA. Systematic and integrative analysis of large gene lists using DAVID bioinformatics resources. *Nat Protoc*. 2009;4(1):44-57.
17. da Huang W, Sherman BT, Lempicki RA. Bioinformatics enrichment tools: paths toward the comprehensive functional analysis of large gene lists. *Nucleic Acids Res*. 2009;37(1):1-13.
18. Szklarczyk D, Morris JH, Cook H, et al. The STRING database in 2017: quality-controlled protein-protein association networks, made broadly accessible. *Nucleic Acids Res*. 2017;45(D1):D362-D368.
19. Shannon P, Markiel A, Ozier O, et al. Cytoscape: a software environment for integrated models of biomolecular interaction networks. *Genome Res*. 2003;13(11):2498-2504.
20. Wang P, Wang Y, Hang B, Zou X, Mao JH. A novel gene expression-based prognostic scoring system to predict survival in gastric cancer. *Oncotarget*. 2016;7(34):55343-55351.
21. Friedman J, Hastie T, Tibshirani R. Glmnet: Lasso and elastic-net regularized generalized linear models. R package versiSon. 2009.
22. Tibshirani R. The lasso method for variable selection in the Cox model. *Stat Med*. 1997;16(4):385-395.
23. Chen B, Khodadoust MS, Liu CL, Newman AM, Alizadeh AA. Profiling tumor infiltrating immune cells with CIBERSORT. *Methods Mol Biol*. 2018;1711:243-259.
24. Kawada JI, Takeuchi S, Imai H, et al. Immune cell infiltration landscapes in pediatric acute myocarditis analyzed by CIBERSORT. *J Cardiol*. 2021;77(2):174-178.
25. Racle J, de Jonge K, Baumgaertner P, Speiser DE, Gfeller D. Simultaneous enumeration of cancer and immune cell types from bulk tumor gene expression data. *eLife*. 2017;6:e26476. https://doi.org/10.7554/eLife.26476
26. Finotello F, Mayer C, Plattner C, et al. quanTIseq: quantifying immune contexture of human tumors. *BioRxiv*. 2017:223180. https://doi.org/10.1101/223180
27. Meylan M, Becht E, Sautès-Fridman C, Reyniès A, Petitprez F. webMCP-counter: a web interface for transcriptomics-based quantification of immune and stromal cells in heterogeneous human or murine samples. *BioRxiv*. 2020. https://doi.org/10.1101/2020.12.03.400754
28. Aran D, Hu Z, Butte AJ. xCell: digitally portraying the tissue cellular heterogeneity landscape. *Genome Biol*. 2017;18(1):220.
29. Li B, Li T. TIMER: Tumor IMmune Estimation Resource. 2016.
30. Yoshihara K, Shahmoradgoli M, Martínez E, et al. Inferring tumour purity and stromal and immune cell admixture from expression data. *Nat Commun*. 2013;4:2612.
31. Liberzon A, Subramanian A, Pinchback R, Thorvaldsdottir H, Tamayo P, Mesirov JP. Molecular signatures database (MSigDB) 3.0. *Bioinformatics*. 2011;27(12):1739-1740. https://doi.org/10.1093/bioinformatics/btr260
32. Liao Y, Wang J, Jaehnig EJ, Shi Z, Zhang B. WebGestalt 2019: gene set analysis toolkit with revamped UIs and APIs. *Nucleic Acids Res*. 2019;47(W1):W199-W205.
33. Zhou C, Pan R, Li B, et al. GPX3 hypermethylation in gastric cancer and its prognostic value in patients aged over 60. *Future Oncol*. 2019;15(11):1279-1289.
34. Wang JY, Yang IP, Wu DC, Huang SW, Wu JY, Juo SH. Functional glutathione peroxidase 3 polymorphisms associated with increased risk of Taiwanese patients with gastric cancer. *Clin Chim Acta*. 2010;411(19–20):1432-1436.
35. Zhang L, Song M, Zhang F, et al. Accumulation of Nicotinamide N-Methyltransferase (NNMT) in cancer-associated fibroblasts: a potential prognostic and predictive biomarker for gastric carcinoma. *J Histochem Cytochem*. 2021;69(3):165-176.
36. Wu M, Hu W, Wang G, Yao Y, Yu XF. Nicotinamide N-methyltransferase is a prognostic biomarker and correlated with immune infiltrates in gastric cancer. *Front Genet*. 2020;11:580299.
37. Chen C, Wang X, Huang X, et al. Nicotinamide N-methyltransferase: a potential biomarker for worse prognosis in gastric carcinoma. *Am J Cancer Res*. 2016;6(3):649-663.
38. Liang L, Zeng M, Pan H, Liu H, He Y. Nicotinamide N-methyltransferase promotes epithelial-mesenchymal transition in gastric cancer cells by activating transforming growth factor-β1 expression. *Oncol Lett*. 2018;15(4):4592-4598.
39. Zou D, Li Z, Lv F, et al. Pan-cancer analysis of NOS3 identifies its expression and clinical relevance in gastric cancer. *Front Oncol*. 2021;11:592761.
40. Wu H, Xu JB, He YL, et al. Tumor-associated macrophages promote angiogenesis and lymphangiogenesis of gastric cancer. *J Surg Oncol*. 2012;106(4):462-468.
41. Svensson MC, Warfvinge CF, Fristedt R, et al. The integrative clinical impact of tumor-infiltrating T lymphocytes and NK cells in relation to B lymphocyte and plasma cell density in esophageal and gastric adenocarcinoma. *Oncotarget*. 2017;8(42):72108-72126.

42. Fristedt R, Borg D, Hedner C, et al. Prognostic impact of tumour-associated B cells and plasma cells in oesophageal and gastric adenocarcinoma. *J Gastrointest Oncol*. 2016;7(6):848-859.
43. Knief J, Reddemann K, Petrova E, Herhahn T, Wellner U, Thorns C. High density of tumor-infiltrating B-lymphocytes and plasma cells signifies prolonged overall survival in adenocarcinoma of the esophagogastric junction. *Anticancer Res*. 2016;36(10):5339-5345.
44. Thompson ED, Zahurak M, Murphy A, et al. Patterns of PD-L1 expression and CD8 T cell infiltration in gastric adenocarcinomas and associated immune stroma. *Gut*. 2017;66(5):794-801.
45. Christina Svensson M, Lindén A, Nygaard J, Borg D. T cells, B cells, and PD-L1 expression in esophageal and gastric adenocarcinoma before and after neoadjuvant chemotherapy: relationship with histopathological response and survival. *Oncoimmunology*. 2021;10(1):1921443.
46. Mansuri N, Birkman EM, Heuser VD, et al. Association of tumor-infiltrating T lymphocytes with intestinal-type gastric cancer molecular subtypes and outcome. *Virchows Arch*. 2021;478(4):707-717.
47. Chiu YM, Tsai CL, Kao JT, et al. PD-1 and PD-L1 Up-regulation promotes T-cell apoptosis in gastric adenocarcinoma. *Anticancer Res*. 2018;38(4):2069-2078.

SUPPORTING INFORMATION

Additional supporting information may be found in the online version of the article at the publisher's website.

How to cite this article: Yin H-M, He Q, Chen J, Li Z, Yang W, Hu X. Drug metabolism-related eight-gene signature can predict the prognosis of gastric adenocarcinoma. *J Clin Lab Anal*. 2021;35:e24085. https://doi.org/10.1002/jcla.24085